Determination of 3D Seismic Performance of Nonstructural Elements in a Collapsed RC Building Considering TBEC-2018

Memduh KARALAR, Murat CAVUSLU*, Necati MERT

Abstract: The majority of the cost of reinforced concrete (RC) buildings is incurred by nonstructural elements (NSEs). Damage to NSEs has been blamed for a large portion of the deaths and damage caused by recent earthquakes. Furthermore, damage to NSEs has a significant impact on a building's ability to function after an earthquake. As a result, studying NSE seismic behaviour is critical for building engineering. RC structures' seismic performance under three-dimensional (3D) earthquakes will be examined in this study. This paper uses a 3D finite element model of the five-story RC structure that collapsed during the 1999 Kocaeli earthquake. In earthquake analyses, NSE materials include bricks, bookcases, bedrooms, armchairs, washing machines, dishwashers, and refrigerators. NSEs are divided into two categories: those that are anchored to the building and those that are not modelled in accordance with the 2018 Turkish Building Earthquake Code, the building's nonstructural anchored and unanchored elements (TBEC-2018). Special spring elements are also used in the bases of these elements when modelling unanchored NSEs. For the 1999 Kocaeli earthquakes on the far and near faults, separate analyses are carried out. 3D nonlinear seismic analyses show that NSEs have a significant impact on the earthquake behaviour of reinforced concrete structures. NSEs should not be neglected when creating a scale model of a real-world building. This means that whether or not NSEs are attached to RC structures has a significant impact on the nonlinear seismic properties of those structures. In addition, a review of the literature reveals that the seismic behaviour of NSEs has not been studied with TBEC-2018. As a result, the findings of this research add something new to the body of knowledge.

Keywords: anchored nonstructural element; far fault earthquakes; near fault earthquakes; seismic design code; unanchored nonstructural element

1 INTRODUCTION

Nonstructural elements (NSEs) in reinforced concrete (RC) structures have become increasingly important in performance-based structural engineering. NSEs have been shown to have a significant impact on RC building functional and economic losses during previous earthquakes [1]. This also emphasizes the importance of anchoring NSEs so that they won't cause damage or injury in the event of an earthquake. The use of anchors to connect bearing elements with NSEs is uncommon in many countries, however. As a result, the NSEs are primarily responsible for the loss of life and property during the earthquake [2-3]. NSEs are critical to a building's long-term viability and account for the majority of its construction costs [4-5]. In recent years, damage to nonstructural systems due to strong ground motions has increased repair costs and lengthened construction times significantly [6-8]. As a result, there has been a noticeable increase in attention paid to NSEs recently. Structural and nonstructural performance must be well coordinated to achieve smooth seismic performance [9-10]. Researchers are only now beginning to understand and explore the significance of NSEs. In the first place, Pantelides et al. were the first to conduct research on NSEs. The nonlinear earthquake behaviour of a single-story commercial building made up of masonry walls, a glass and aluminium workshop, and a steel bar joist metal deck roof system is investigated using the ABAQUS and SAP 90 programs in this study. Tests on architectural glass in plane drifts are more important than on other nonstructural elements; it is emphasized. Window glass panels were studied by Sucuolu and Vallabhan for their seismic behaviour [12]. Window panes exposed to seismic loading have been subjected to an analytical procedure that determines their in-plane deformation capacity and out-of-plane resistance. Xue et al. used a performance-based seismic design code to apply direct displacement techniques to the structures. The nonstructural damage is limited by the structural drift limit in this technique, which designs NSEs to take acceleration or displacement into account. An investigation

by Ji et al. found that the most significant damages were found in the coupling beams and NSEs of a high-rise building with a novel hybrid coupled walls. There was a pinched hysteresis model validated by experimental laboratory results in Smith and Vance's model of nonlinear nonstructural architectural wall behaviour [15-16]. Seismic performance assessment of NSEs in unreinforced clay brick masonry buildings was carried out by Derakhshan et al. In Australia and New Zealand, NSEs include parapets, chimneys, and other out-of-plane-loaded facades common in older low-rise buildings built before the 1940s. Observations revealed that NSE seismic performance estimates derived from these new datasets were accurate [17]. NSEs attached to multistory buildings were studied for their seismic response by Pardalopoulos and Pantazopoulou. When a building is at its maximum lateral roof displacement, the seismic behaviour of NSEs is seen to be dependent on the deformed shape of the supporting structure [18]. Furthermore, a new seismic design procedure for NSEs is proposed, and this important procedure improves the predictions of a relative displacement floor response spectrum by constraining its ordinates at long nonstructural periods to the expected peak absolute displacement of the floor [19]. NSEs subjected to floor accelerations were studied by Obando and Lopez-Garcia for inelastic displacement ratios. To characterize the inelastic displacement ratios (IDRs) of nonlinear structural elements (NSEs) that are affected by far-field ground accelerations, researchers used linear analysis on multistory building structures. For the design of acceleration-sensitive NSEs, Anajafi and Medina used data from instrumented buildings to evaluate ASCE 7 equations. The study's primary goal is to validate previous studies that found that the ASCE 7 equation needed to be revised when using overly simplified generic linear and nonlinear numerical models when using instrumented buildings and models of code-based designed buildings [21]. Anajafi et al. designed acceleration-sensitive nonstructural components using inelastic floor spectra (NSCs). There are two parameters used to quantify the effects of NSCs' inelasticity on seismic-induced force and

displacement demands: response modification factor and inelastic displacement ratio [22]. Using a cost-performance evaluation, Bianchi et al. compared traditional building systems with low-damage structural and nonstructural building systems. In a cost/performance-based evaluation of RC buildings, damage control solutions for structural components and NSEs such as heavy/light facades, heavy/light partitions, and suspended ceilings were compared to alternative combinations of traditional and low damage technologies. In these specific cases, parametric analyses confirm that the integrated low-damage structural/nonstructural system can save 150 to 300 euro/m^2 over the building's 50-year life and reduce downtime by 2 to 7 months at the ultimate limit state [23]. Sullivan looked at how quickly buildings could be repaired after an earthquake and what role NSEs played in that. Following a severe earthquake, time and repair costs could be saved significantly by considering potential inspection and repair needs during concept design, with significant socio-economic benefits for the community [24]. Electrical equipment, a piping system, and a commonly used suspended ceiling structure were all tested using shake tables by Qi et al. for seismic performance. Under earthquake excitation, experimental results showed that the two-elevation ceiling system worked well. During the shaking, no panels fell, or the entire system collapsed. A strong temporary-positioning-bracing bar (TPBB) was found to be critical in reducing the relative displacement between two ceiling elevations and in ensuring the integrity of both ceiling elevations within the ceiling system [25]. After that, nonstructural damages caused by the 2016 Central Italy earthquake were analyzed. This earthquake's damage is primarily due to excessive lateral drifts of the structures, which can be traced back to the masonry infill and partition walls. The interaction with the structures and the lack of bracing systems caused significant damage to the ceiling systems, especially to the suspended light vaults. In NSEs that are acceleration-sensitive, such as chimneys, appendages, and roof tiles, inadequate connections or bracing systems lead to poor seismic performance [26]. Damage to NSEs can be costly due to the time and money required to repair it, and the findings confirmed that NSE damage could also pose a significant risk to people's lives. The 2016 Kaikura earthquake occurred at a time when many buildings were not occupied, and this was brought to light [27]. According to Isik et al., the amount of damage to masonry structures increased due to the absence of engineering services. The amount of damage to RC structures increased as a result of insufficient reinforcement and concrete strength, as well as poor dimensions and detailing. In addition, negative parameters that weaken structures' defence mechanisms should be considered for earthquake-resistant structural design; it was noted [28]. According to Yurdakul et al., NSEs in the ground story suffer more damage as a result of higher inter-story drift requirements. NSEs are also vulnerable to damage even in earthquakes of low intensity because of a lack of inherent strength and stiffness [29]. The 2018 Turkish Building Earthquake Code (TBEC-2018) has also been the subject of numerous studies [30-37]. When these studies are examined, it becomes clear that TBEC-2018 was not used to investigate the seismic behaviour of NSEs. When comparing this study to others, it should be noted that TBEC-2018 was used to determine the effects of NSEs on the seismic behaviour of reinforced concrete structures (RC structures). To add to their work,

Karalar and Çavuşli looked into the seismic performance of NSEs based on Eurocode 8 and the International Building Code [43, 44]. In addition, Cavuslu investigated the seismic behavior of nonstructural elements both experimentally and numerically and revealed the effects of nonstructural elements on the seismic behavior of RC structures [44].

There are numerous studies in the literature on the seismic performance of nonstructural elements, as can be seen from these examples. There has not been much research done on the seismic effects on 3D far fault and near-fault building performance of anchored and unanchored NSEs before, according to TBEC-2018. As a result, this research is crucial in bridging the knowledge gap. This research examines the nonlinear seismic behaviour of RC buildings in three dimensions when subjected to NSEs, far fault earthquakes, and earthquakes close to the building's location. The Sakarya-Turkey Kocaeli earthquake in 1999 caused this RC building to crumble. Three-dimensional (3D) modelling was done using SAP2000 software [39] for this structure. To ensure accuracy, all bearing elements (beams, columns, and the foundation) have been modelled using the original project's specifications, including the original concrete grade. The 3D numerical analyses utilize the 1999 Kocaeli earthquake's far fault and near-fault components. To begin, only the structural elements of an RC structure are taken into account when performing an analysis of it (without NSEs). Finally, the library structure is used to model NSEs. Brick is treated as a non-significant element (NSE) in the numerical analysis because it is considered to be a common household item. These nonstructural forces are implemented into a 3D model by considering the main locations of NSEs throughout the building, and the vertical and horizontal nonstructural forces for each floor are separately calculated according to this standard. Afterwards, the structure is scrutinized with an eye toward anchored NSEs. Last but not least, special springs are defined below NSEs, and the building is examined in light of unanchored NSEs. The seismic displacements, accelerations, and pseudo-spectral acceleration-velocity behaviour of the building are all compared in detail using 3D numerical analysis results. RC structures' seismic behaviour has been proven by all analyses, and it is highly recommended that NSEs be included in the structural analysis as a result. In addition, the results of this research show that whether NSEs are anchored to a structure or not, the seismic behaviour of RC structures changes.

2 FORCE-BASED SEISMIC DESIGN OF NONSTRUCTURAL ELEMENTS

Nonstructural elements (NSEs) have not been taken into account in structural modelling in many countries. This is due primarily to the widespread belief that NSEs are void of power. Recent studies, on the other hand, have found that NSEs have a significant impact on a structure's seismic behaviour, and the significance of NSEs is only now being understood. The seismic behaviour of NSEs is designed primarily to protect people and other living things from harm. Fixing NSEs to the supporting structure is one way of accomplishing this, as is reducing the likelihood of internal damage to NSEs, especially in critical

infrastructure. Many countries' seismic design requirements are based on the premise that natural seismic events (NSEs) can be dynamically separated from the underlying structural system. Prior to considering interactions with nonstructural components, the seismic floor behaviour of the supporting structure is determined for this approach. To begin with, seismic design begins by calculating the design forces of each element in horizontal and/or vertical directions and then applying these seismic forces to NSE's centre of mass. These seismic design standards can be found in places like North America, Europe, New Zealand, and Turkey. In order to calculate the equivalent design forces of NSEs, you multiply the NSE's mass by the expected horizontal and/or vertical accelerations in the NSE's centre of mass during the seismic event. There is an important factor applied to seismic design forces for NSEs, similar to structural components (I). There is also a response modification factor for nonlinear responses and over the strength of NSEs divided by these earthquake design forces.
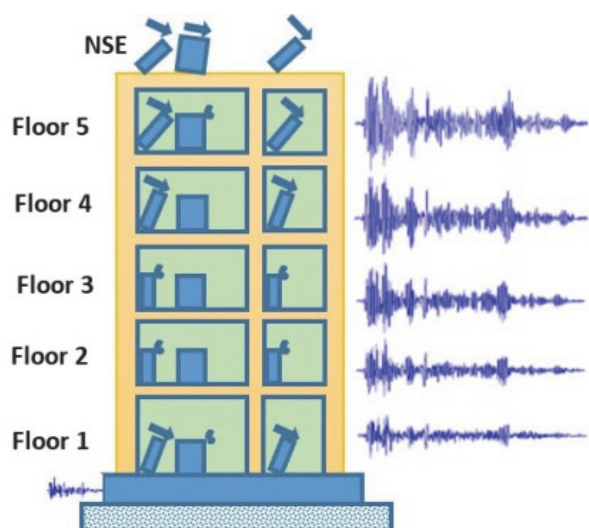

Figure 1 View of NSC in the structure according to Force Method [27]
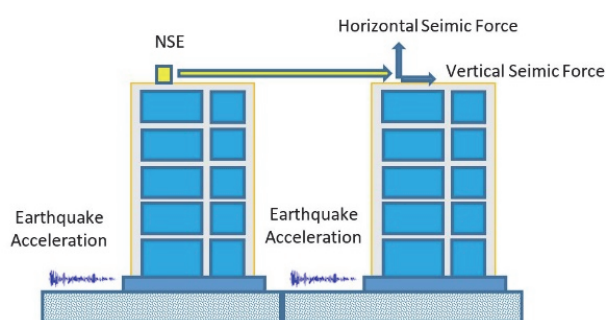

Figure 2 Acceleration histories at different floors [27]

With the advent of new national seismic force design provisions, many countries (including the United States and Turkey) now have their own guidelines for NSE seismic force design. These provisions allow NSEs to be modelled using seismic force-based design. It is recommended that NSEs be modelled in the structure as if they are horizontal/vertical forces while using this design method (Fig. 1). Separate formulations have been created for NSE forces within these provisions. When an earthquake affects a building's foundation, it is easy to see that the earthquake acceleration values vary from floor to

floor (Fig. 2). NSE force formulations are calculated separately on each floor of the structure according to these standards.

3 TURKISH BUILDING EARTHQUAKE CODE (TBEC-2018) FOR NONSTRUCTURAL ELEMENTS

The Turkish earthquake code was completely rewritten in 2018 to include all of the previously unaccounted-for situations. Turkish earthquake code requires earthquake calculations for all nonstructural elements (NSEs), mechanical and electrical equipment and connections to the structure, as well as all types of protrusions (such as balconies, parapets, chimneys and cantilevers) and facade and partition panels. Fasteners (such as welds, bolts, dowels, and rivets) connecting the NSE to the structure under the influence of an earthquake will not take additional capacity due to friction into account. Eq. (1), [38] defines the equivalent earthquake load acting horizontally at the NSE center.

$$F_{ie} = \frac{m_e A_{ie} B_e}{R_e} \tag{1}$$

In this equation, m_e - weight of NSE, A_{ie} - the greatest total acceleration on the floor under earthquake motion, B_e - the magnification factor applied to the NSE, R_e - Behaviour coefficient defined for NSE. According to TBEC-2018, special seismic values are defined for B_e and R_e, and these seismic values can be provided from Tab. 1 (this table is obtained from TBEC-2018) [38].

Table 1 Amplification and Behaviour Coefficients for Nonstructural elements

Nonstructural elements	B_e	R_e
Nonstructural masonry interior walls and partitions	1.0	1.5
Other nonstructural interior walls and partitions	1.0	2.5
Cantilever elements without lateral support or with lateral support below the centre of gravity	2.5	2.5
Cantilever elements with lateral support above the centre of gravity	1.0	2.5
External walls and connections	1.0	2.5
Facade cladding panels	1.0	1.5
Roof floors independent of the building system	2.5	3.5
Suspended ceilings	1.0	2.5
Billboards	2.5	2.5
Other rigid architectural elements	1	2.5
Other flexible architectural elements	2.5	2.5

$$A_{ie} = (R / I)\left(\frac{2\pi}{T_p}\right)^2 u_i \tag{2}$$

In this Eq. (2), R - behaviour coefficient defined for building, I - building importance factor, T_p - the natural vibration period of the building in the direction of the earthquake considered, u_i - horizontal displacement calculated according to reduced earthquake loads at any floor of the building in the direction of the earthquake considered [38].

4 GENERAL INFORMATION OF RC BUILDING

NSE seismic effects on the earthquake behaviour of reinforced concrete buildings (RC buildings) are

investigated using the finite element method in this study. An RC building in Sakarya, Turkey, constructed in 1956, was chosen for 3D numerical analyses for this purpose (Fig. 3). This building has five stories and is right next to the sea. It has been in continuous use for 44 years. People who live in the building can store extra goods on the ground floor. All of the other floors are in use. Fig. 4 depicts the most critical areas of these floors. Each floor has two balconies and polygonal geometry. The structure's foundation is of type B. A devastating earthquake struck in 1999 and completely demolished this structure. In addition, AFAD 2021 was used to obtain the earthquake parameters based on the location of the building [40]. It weighs 0.668 grams and travels at 49.719 centimetres per second at location PGA (475).

Figure 3 a) Before and b) after views of RC structure [41-43]
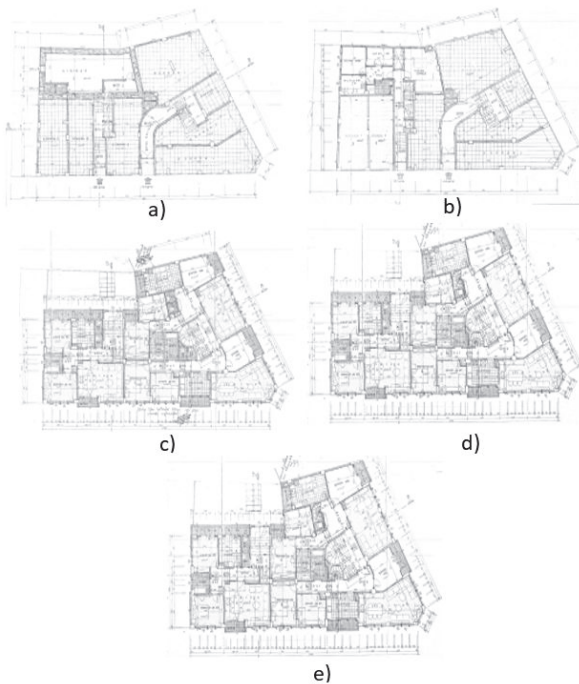
Figure 4 Sections of structure floors a) first-floor; b) second floor; c) third floor; d) fourth floor; e) fifth floor [42, 43]

5 3D MODELLING STRUCTURAL AND NONSTRUCTURAL COMPONENTS OF RC BUILDING AND GROUND MOTIONS

Nonstructural elements' seismic displacement and acceleration performance will be examined in this study (NSEs). RC buildings that collapsed during a powerful earthquake are used for 3D modelling in this case. 6 columns are defined in the software when modelling this RC structure, with sizes of 30 × 75 cm, 30 × 95 cm (30 × 60 cm), 35 × 75 cm (35 × 75 cm), 35 × 90 cm (35 × 115 cm) and 35 × 115 cm (35 × 90 cm) respectively. A circular

column with a 65 cm diameter also exists in the design. The 3D model then uses beams with dimensions of 25 × 40 cm, 30 × 40 cm, and 30 × 45 cm. The C20 concrete class is used for columns and beams, and this value can be found in the original structure plan. The compressive strength of this concrete is about 19.4 N/mm², which indicates that it is of poor quality. There are two distinct shear walls in the RC structure, each measuring 20 cm in thickness. Additionally, all floors have a 20 cm thickness to their floor coverings. The structure has five floors with a total height of 3 m. It is necessary for a model to include elements known as "FRAMEs" (such as columns and beams). After that, the building's floors are created, and its "AREA" components are meshes. The structure has a rigid diaphragm assigned to it so that during an earthquake, all of the elements move together. The movement of the structure's foundation is restricted by fixed supports as a mass source is defined in software using dead, live, and earthquake loads. As a next step, only structural elements in accordance with the direct integration solution type are taken into account in nonlinear time history analyses. The Hilber-Hughes-Taylor method, with gamma and beta values of 0.5 and 0.25, is used in the 3D analyses for this purpose.
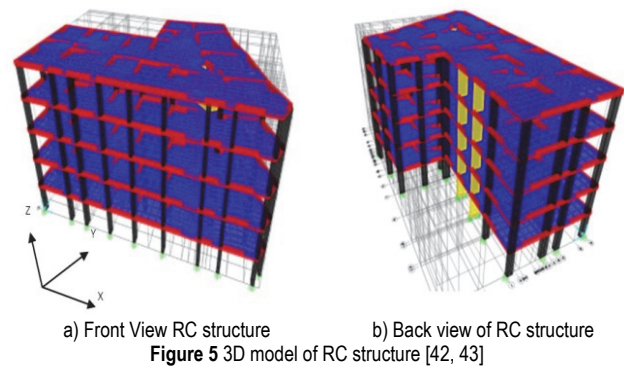

a) Front View RC structure   b) Back view of RC structure
Figure 5 3D model of RC structure [42, 43]

Fig. 5 depicts the structure's 3D model in three dimensions. NSEs are defined to the structure using spring elements after structural components have been created in accordance with the original structure project. Structures (brick, bookshelf, bedroom, armchair) are built in accordance with the original location of nonstructural building elements (such as a washing machine, dishwasher, and refrigerator). RC building's total NSE weight is 7 percent of the total building weight. Section 6.1.3 of TBEC-2018 has a special situation for situations like this. NSE will be regarded as a building carrier system if its weight exceeds 10% of the floor's total weight, according to this special circumstance. To estimate the seismic loads of NSEs, the USGS uses the TBEC-2018 model. Nonstructural loads are defined in software based on the original locations of NSEs in the structure after the calculations have been completed (Fig. 6). RC structure is assumed to be the anchor for these NSE loads. An anchored NSE has extremely high spring coefficients. Apart from that, NSEs are assumed to be unanchored from the RC structure, and special seismic springs are defined to sit beneath these unanchored NSEs for this purpose (Fig. 7). A "GAP" link/support is used, and spring coefficients for unanchored NSEs are presumed to be close to zero. GAP is assumed to be an infinitesimal distance between NSE and nodal point.
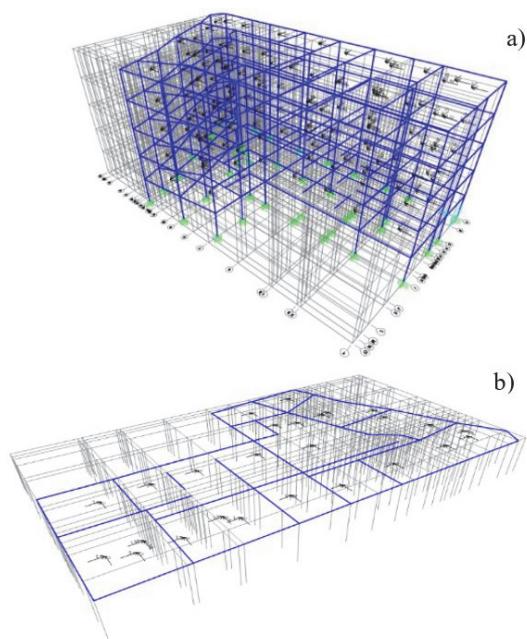
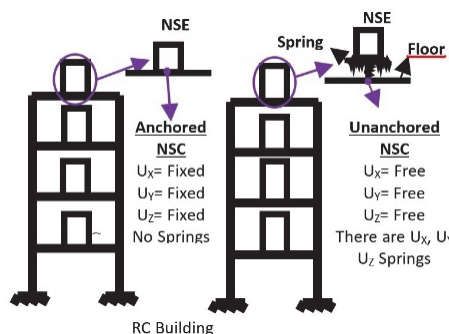**Figure 6** Nonstructural element loads for a) all floors; b) only last floor

Figure 7 Modelling of anchored and unanchored NSEs in seismic analyses [42, 43]

Fig. 7 shows that the anchored NSE's freedoms (U_X, U_Y, and U_Z directions) are "fixed". The freedoms of unanchored NSE are also "free" (U_X, U_Y, U_Z directions). NSEs that are anchored and unanchored are referred to as a super dead load, respectively, by the software.
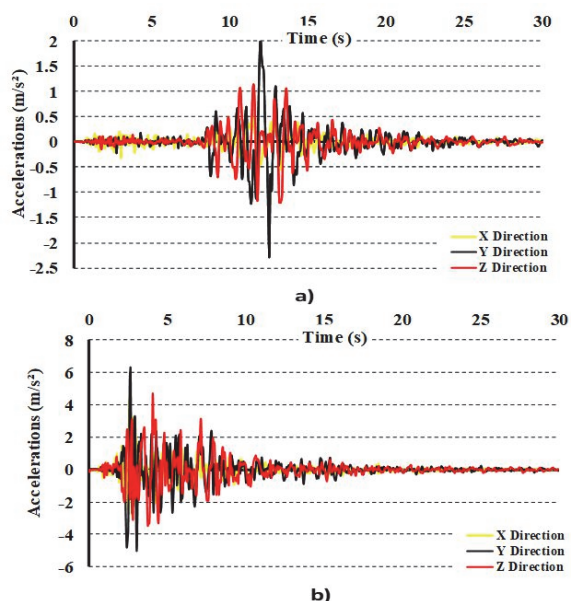

Figure 8 Time history graphics of 1999 Kocaeli earthquake a) far fault; b) near fault ground motion

Fig. 8 depicts the magnitude 8 acceleration of the 1999 Kocaeli earthquake's far fault and near-fault ground motions. As shown in Fig. 8, the maximum accelerations of earthquakes on the far fault and near-fault are 2.26 m/s² and 6.26 m/s², respectively.

6 3D NONLINEAR SEISMIC ANALYSIS RESULTS

When seismic modelling RC structures, many scientists ignore nonstructural elements (NSEs). Even though NSEs are not able to support any weight, they can still alter the seismic behaviour of structures when an earthquake occurs. To better understand earthquake behaviour in structures, this study examined the impact of NSEs. In this section, the earthquake behaviour of a three-dimensional RC building model is discussed by taking into account NSEs. NSEs and TBEC-2018 are taken into account when conducting seismic analyses. Seismic design loads for NSEs are calculated using TBEC-2018, as shown in Tab. 2.

Table 2 Seismic loads of nonstructural elements

Non-structural elements	Floor	Non-structural element loads for TBEC-2018
Brick	First	176
	Second	234
	Third	281
	Fourth	341
	Fifth	396
Washing Machine	First	51
	Second	69
	Third	94
	Fourth	119
	Fifth	131
Dish Washer	First	50
	Second	70
	Third	85
	Fourth	97
	Fifth	118
Refrigerator	First	58
	Second	79
	Third	94
	Fourth	117
	Fifth	126
Armchair	First	37
	Second	53
	Third	67
	Fourth	84
	Fifth	91
Bedroom	First	132
	Second	214
	Third	276
	Fourth	328
	Fifth	386
Bookcase	First	58
	Second	75
	Third	93
	Fourth	121
	Fifth	136

Table 3 Situations of RC structure for 3D seismic analyses

Case	The situation of RC structure
Case 1	Structure with anchored NSEs
Case 2	Structure with unanchored NSEs

As can be seen in Tab. 3, the RC structure is examined in two different scenarios (structures with and without anchored NSEs). In order to meet this standard, far-near fault earthquakes are compared numerically in terms of their *x*, *y*, and *z* displacements as well as pseudo-spectral

accelerations-velocities. Additionally, with this standard in mind, the graphics compare structures with and without anchored NSEs. The results of a nonlinear 3D analysis show that the effects of anchored and unanchored NSEs on the seismic behaviour of RC structures are vastly different. The distance between an earthquake fault and an RC structure has also been found to affect the 3D earthquake behaviour of RC structures. Figs. 9 to 24 show the results of the 3D earthquake analysis. The top floor of the RC structure experienced the greatest X displacement during the far fault earthquake, as shown in Fig. 9.
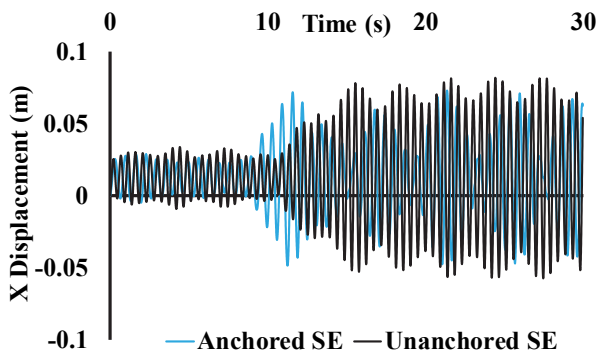
Figure 9 Time history X displacement analysis results for far fault earthquake

It is Case 1 that yields the largest X displacement, which is numerically equal to 78 mm. Comparing Case 2 to Case 1, the max X displacement is smaller (71 mm). Within the first 10 seconds of the earthquake's occurrence, only very small X displacements were detected. Fig. 10 depicts the numerical results of an earthquake near a fault. Figs. 9 and 10 show that the near-fault earthquake had greater X displacements than the far-fault earthquake. Case 1 has a maximum X displacement of 198 mm for structures with anchored NSE that are near the fault (Fig. 10).
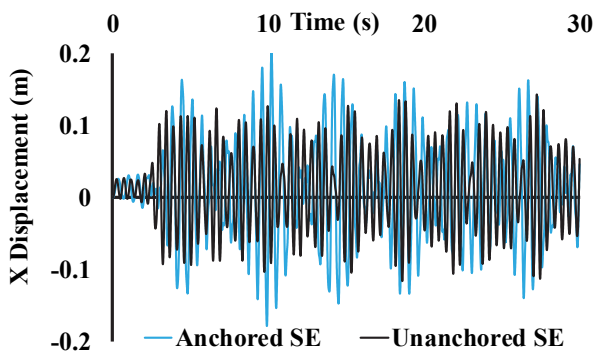

Figure 10 Time history X displacement analysis results for the near-fault earthquake

As an additional point of interest, Case 2's highest possible vertical displacement is 141 millimeters. These findings show that anchored NSEs cause greater max X displacements for earthquakes near faults than unanchored NSEs. Fig. 11 shows the RC structure's greatest Y displacement during the far fault earthquake. Fig. 11 shows that for Case 1 (the structure with the anchored NSEs), the maximum Y displacement is larger, at 94 mm. Unanchored NSE structures have lower Y displacements. Fig. 12 shows the structure's 1999 Kocaeli near-fault earthquake's largest Y displacement results in great detail. When comparing Figs. 11 and 12, the Y displacements for far fault earthquakes are smaller than the Y displacements for near-fault earthquakes. Fig. 12 shows that during a far fault earthquake, the structure with anchored NSE has the largest Y displacement at the top floor, and the largest Y displacement for the structure with anchored NSE is 331 mm. The largest Y displacement for unanchored NSEs is 312 mm.
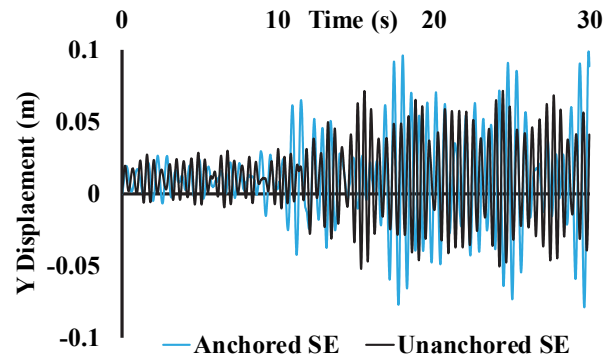

Figure 11 Time history Y displacement analysis results for far fault earthquake
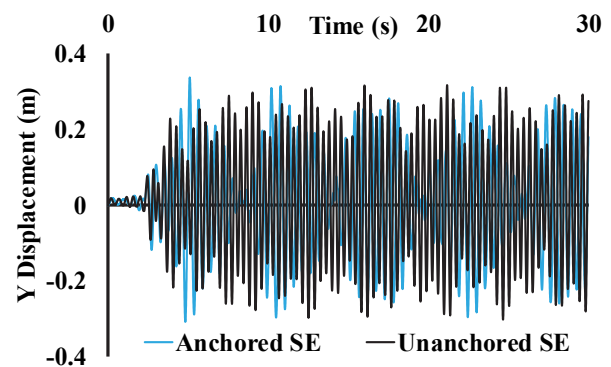

Figure 12 Time history Y displacement analysis results for the near-fault earthquake

Fig. 13 shows the time-dependent seismic Z displacement results at the RC building's top floor during the far fault earthquake. Case 2 had greater Z displacements than Case 1, as shown in Fig. 13. In the event of a far fault earthquake, structures with unanchored NSEs will experience a maximum Z displacement of 2.1 mm. Figs. 13 and 14 show that the near-fault earthquake has larger Z displacements when compared. Fig. 14 shows that during the near-fault earthquake, the structure with anchored NSEs had larger Z displacements at the top floor than the rest of the structure (Case 1). Case 1 has a maximum Z displacement of 7.92 mm due to an earthquake near the fault.
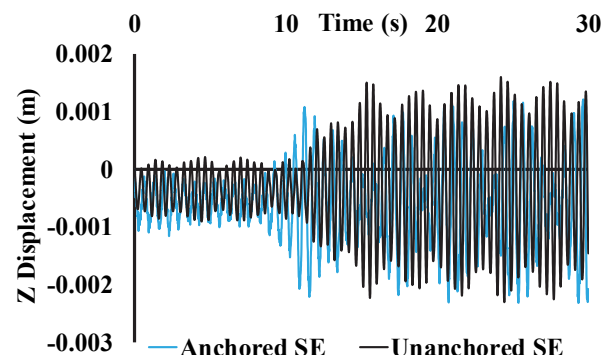

Figure 13 Time history Z displacement analysis results for far fault earthquake
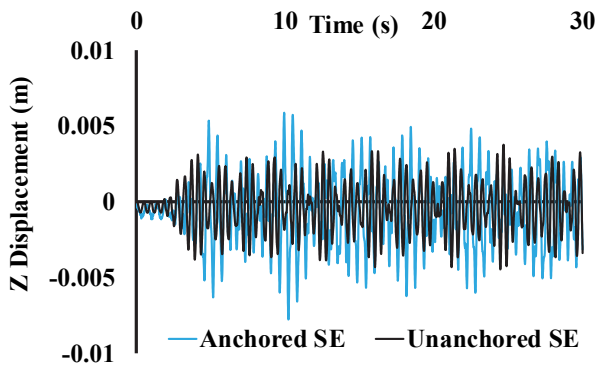
Figure 14 Time history Z displacement analysis results for the near-fault earthquake

Moreover, the effective relative storey drifts are controlled according to Eq. (3) (section 6.3.2 of TBEC-2018). h_x and h_y show the height of the upper and lower connection points of NSE from the relevant floor base and $\dfrac{\delta_{i,\max}^{(X)}}{h_i}$ indicate the maximum allowable relative floor drift ratio.

$$\delta_e^{(X)} \leq (h_x - h_y)\frac{\delta_{i,\max}^{(X)}}{h_i} \tag{3}$$

Pseudo-spectral acceleration results are shown in Figs. 15 and 16 for the point on the top floor of the structure where the greatest displacement occurred during far and near-fault earthquakes. Fig. 15 shows that during a far fault earthquake, structures with unanchored NSE have a higher pseudo-spectral acceleration value. With an unanchored NSE, the maximum pseudo-spectral acceleration is 119.475 m/s². The structure with anchored NSEs experienced a maximum pseudo-spectral acceleration of 41.238 m/s² during the far fault quake.
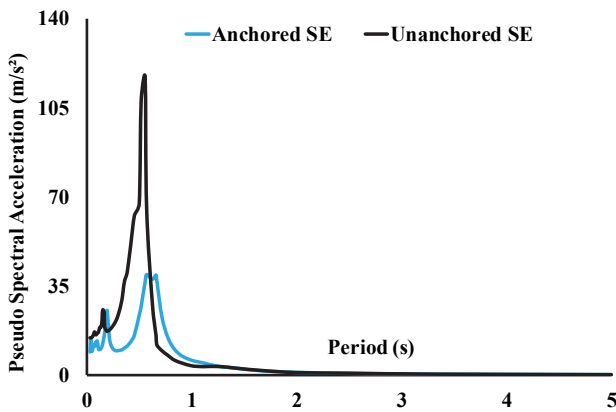

Figure 15 Time history pseudo-spectral acceleration results for far fault earthquake

For the point on the top floor of the structure that experienced the greatest displacement during a near-fault earthquake, the pseudo-spectral acceleration value is shown in Fig. 16. This numerical value of 181.549 m/s² is obtained for the structure with anchored NSE during the earthquake near the fault. The structure with unanchored NSEs has smaller pseudo-spectral acceleration values. In light of this result, it is clear that the fault distance has an impact on the spectra of RC structures.
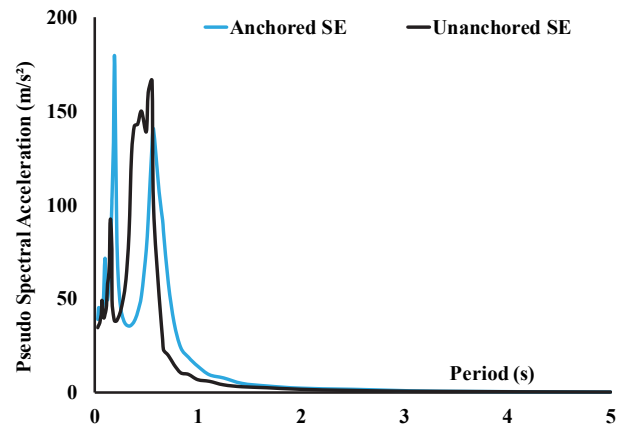

Figure 16 Time history pseudo-spectral acceleration results for the near-fault earthquake

There are comparisons made between structures with and without anchored NSEs in Fig. 17, showing pseudo-spectral velocity results for the point on the top floor of the structure where the largest displacement occurred during the far fault earthquake. The structure with unanchored NSEs, as shown in Fig. 17, has a higher pseudo-spectral velocity value. Case 1 has a maximum pseudo-spectral velocity of 4.208 m/s.
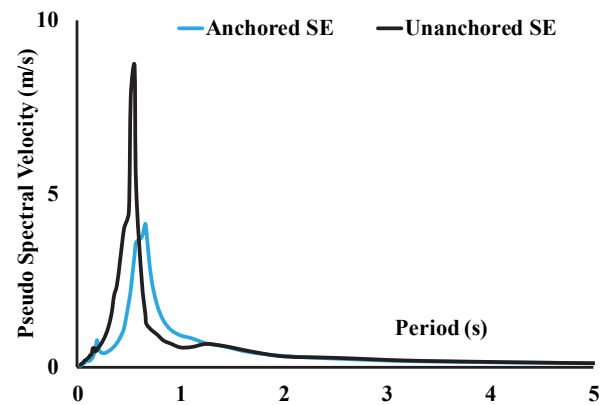

Figure 17 Time history pseudo-spectral velocity results for far fault earthquake

Fig. 18 shows that near-fault earthquakes have higher pseudo-spectral velocity values, which can be seen when looking at the graph in more detail. When comparing Cases 1 and 2, the pseudo-spectral velocity values for Case 1 are higher. The effect of anchoring or not anchoring the NSE to the structure on the seismic behaviour of the structure can clearly be seen from these 3D numerical results.
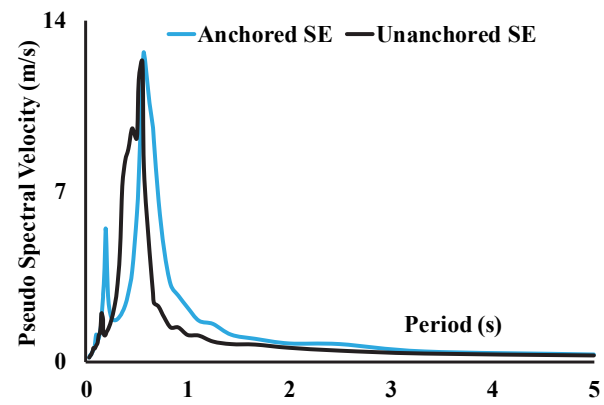

Figure 18 Time history pseudo-spectral velocity results for the near-fault earthquake

Fig. 19 shows that during a far fault earthquake, the structure's top floor with unanchored NSEs experiences higher X acceleration values than floors with anchored NSEs. In the case of the unanchored NSE structure, the maximum X acceleration is 13.189 m/s^2.
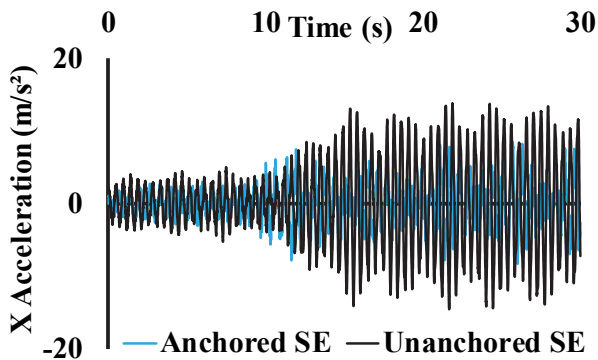

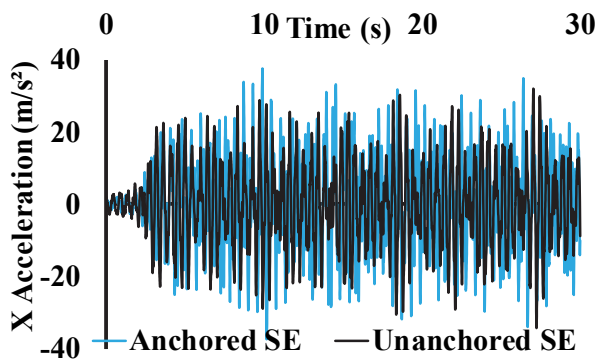**Figure 19** Time history X acceleration results for far fault earthquake

Figure 20 Time history X acceleration results for the near-fault earthquake

For Case 1, higher X acceleration values are observed on the top floor of the structure, according to Fig. 20, and numerical results of the near-fault earthquake are presented for Case 1 and Case 2. On the top floor of the structure with unanchored NSE, 33.189 m/s^2 is the highest X acceleration recorded. When comparing Figs. 19 and 20, it becomes clear that RC structures experienced more X acceleration values during earthquakes that occurred near the fault than during earthquakes that occurred far from the fault. When an earthquake occurs far or near a fault, these time-dependent Y acceleration values can be seen graphically in Figs. 21 and 22.
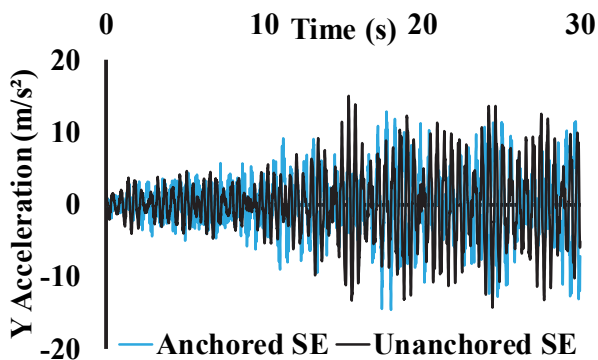

Figure 21 Time history Y acceleration results for far fault earthquake

Fig. 21 shows that during the far fault earthquake, Case 2 had the highest Y acceleration value of 17.382 m/s^2. When comparing Figs. 21 and 22, it becomes clear that the

top floor of the RC structure experiences greater Y acceleration during earthquakes near the fault. In addition, the structure with an anchored NSE has higher Y acceleration values than the structure without an anchored NSE during the fault earthquake (Fig. 22).
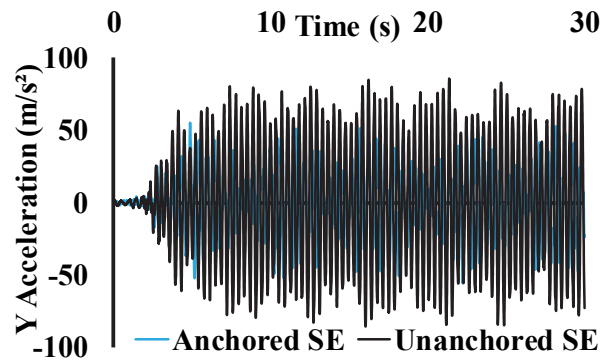

Figure 22 Time history Y acceleration results for the near-fault earthquake

Figs. 23 and 24 show the Z acceleration results for the point on the building's top floor where the largest Z displacement occurred after accounting for earthquakes on the far fault and earthquakes on the near-fault.
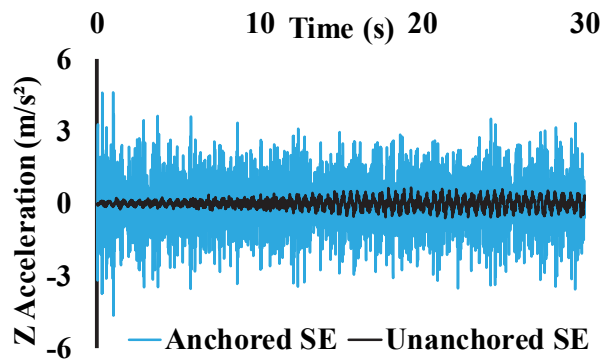

Figure 23 Time history Z acceleration results for far fault earthquake
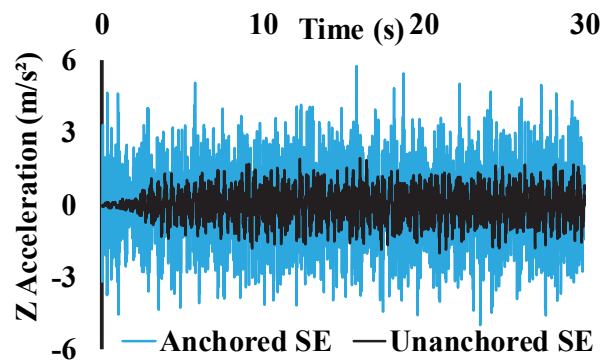

Figure 24 Time history Z acceleration results for the near-fault earthquake

Fig. 23 shows that for a far fault earthquake in Case 1, the Z acceleration values are higher. The building's top floor has anchored NSEs, which results in a maximum Z acceleration of 4.817 m/s^2. Fig. 24 shows that the near-fault earthquake has higher Z accelerations than the far fault earthquake (Fig. 24). Structures with anchored and unanchored NSEs have vastly different Z acceleration values. RC structures' 3D earthquake behaviour can be deduced from the seismic analysis results whether NSE anchoring is used or not. Tab. 4 displays all of the data.

Table 4 3D numerical results

		Far Fault Earthquake	Near Fault Earthquake
Max X Displacement (mm)	Anchored	78	198
	Unanchored	71	141
Max Y Displacement (mm)	Anchored	94	331
	Unanchored	67	312
Max Z Displacement (mm)	Anchored	1.9	7.92
	Unanchored	2.1	5.1
Max Spectral Acceleration (m/s²)	Anchored	41.2	181.5
	Unanchored	119.4	163.4
Max Spectral Velocity (m/s)	Anchored	4.2	13.8
	Unanchored	8.9	13.1
Max X Acceleration (m/s²)	Anchored	11.9	25.9
	Unanchored	13.1	33.1
Max Y Acceleration (m/s²)	Anchored	15.4	88.4
	Unanchored	17.3	81.6
Max Z Acceleration (m/s²)	Anchored	4.8	5.8
	Unanchored	0.8	1.9

7 CONCLUSIONS

Nonstructural elements' (NSEs') 3D nonlinear seismic hazard performance is assessed in light of TBEC-2018 in this study. Furthermore, special seismic spring elements are used to examine the 3D seismic hazard effects of unanchored NSEs on nonlinear earthquake behaviour in RC structures. The RC structure is modelled with anchored and unanchored NCs, and 3D seismic performance analyses are carried out for the 1999 Kocaeli earthquake's far fault and near-fault components (fault distances to structure: 85 km, 11 km). The numerical analyses classify seven different pieces of furniture as non-constants (NCs). In accordance with TBEC-2018, seismic loads on NCs are calculated and then applied to a 3D model of an RC structure. Seismic effects on earthquake behaviour of RC structures according to TBEC-2018 have not been studied in detail, according to literature. That is why this research is critical in identifying this shortcoming. The following significant findings came out of this research:

- The results show that near-fault earthquake analyses yield more X and Y velocities as well as Z velocities, accelerations, and pseudo-spectral velocity-accelerations than far fault analyses. RC structures' earthquake behaviour is shown to be affected by the distance to faults in this study. Building damage increases in direct proportion to the distance from the fault centre to the centre of the structure.
- For all numerical analyses, the highest level of structure height exhibits the largest displacements and accelerations.
- The seismic behaviour and structural safety of RC structures depend greatly on nonstructural elements. When simulating an RC structure, it is critical that NSEs are taken into consideration.
- The earthquake behaviour of RC structures changes significantly depending on whether NSEs are anchored to the structure or not. During an earthquake, NSEs that are attached to a structural element cause greater seismic displacements in that element. So the anchored NSEs to the structure both keep people and property safe during an earthquake while also increasing seismic displacements. As a result, when simulating an RC building, remember to include anchored NSEs.
- Case 1 has the largest X and Y displacements for earthquakes far from the fault and near the fault (structure with anchored NSE). A far fault earthquake's largest X displacement is 78 millimeters, near-fault earthquakes have a depth of 198 millimeters. For example, the largest Y displacement in the far fault

earthquake is 94 millimeters in Case 1. This is 331 millimeters for a near-fault earthquake. A far fault earthquake can cause a Z displacement of up to 2.1 millimeters in Case 2. (structure with unanchored NSEs). Case 1 shows a maximum Z displacement of 7.92 mm during the near-fault earthquake.

- 119.4 m/s² is the maximum pseudo-spectral acceleration for Case 2 in a far fault earthquake. When an earthquake occurs on a far fault, the highest pseudo-spectral acceleration measured is 41.238 m/s². In addition, the highest numerical value of 181.549 m/s² is obtained for Case 1 for the near-fault earthquake for pseudo-spectral acceleration.
- Case 2 shows more X acceleration values for the far fault earthquake, with a maximum X acceleration of 13.189 m/s². In addition, more X acceleration values are found for Case 1 on the top floor of the structure for earthquakes near the fault. Case 2's maximum X acceleration was 33.189 m/s² on the building's top floor.
- The building's non-structural elements are not attached to it in any way. Higher acceleration values were found in the structure with unanchored NSEs, as demonstrated by this research. As a result, the structure underwent larger deformations. The structure would be less likely to deform if the NSEs were anchored to it, allowing it to stand.

8 REFERENCES

[1] Pürgstaller, A., Gallo, P. Q., Pampanin, S., & Bergmeister, K. (2020). Seismic demands on nonstructural components anchored to concrete accounting for structure-fastener-nonstructural interaction (SFNI). *Earthquake Engineering and Structural Dynamics*, *49*, 589-606. https://doi.org/10.1002/eqe.3255

[2] Taghavi, S. & Miranda, E. (2003). *Response assessment of nonstructural building elements*. PEER report 2003/05. Berkeley: Pacific Earthquake Engineering Research Center, College of Engineering.

[3] Retamales, R., Davies, R., Mosqueda, G., & Filiatrault, A. NEES R (2009). Grand Challenge project: simulation of the seismic performance of nonstructural systems: experimental phase 1: Seismic performance of partition wall subsystems. *Proccedings of the NEES 7th Annual Meeting*, Honolulu, Hawaii.

[4] Giuseppe, M. D. G., Martin, S. W., & Anthony, B. (2018). Seismic performance assessment of Eurocode 8-compliant concentric braced frame buildings using FEMA P-58. *Engineering Structures*, *155*, 192-208. https://doi.org/10.1016/j.engstruct.2017.11.016

[5] Danilo, D., Gennaro, M., & Edoardo, C. (2021). Seismic damage assessment of unanchored non structural components taking into account the building response. *Structural Safety*, *93*. https://doi.org/10.1016/j.strusafe.2021.102126

[6] Fierro, E. A., Miranda, E., & Perry, C. L. (2011). Behaviour of non-structural components in recent earthquakes. *Architectural Engineering Conference (AEI) 2011*, 369-77. https://doi.org/10.1061/41168(399)44

[7] Dhakal, R. P. (2010). Damage to non-structural components and contents in 2010 Darfield earthquake. *Bulletin of the New Zealand Society for Earthquake Engineering*, *43*, 404-11. https://doi.org/10.5459/bnzsee.43.4.404-411

[8] Miranda, E., Mosqueda, G., Retamales, R., & Pekcan, G. (2012). Performance of non-structural components during

the 27 February 2010 Chile earthquake. *Earthquake Spectra*, *28*, 453-71. https://doi.org/10.1193/1.4000032

[9] Pürgstaller, A., Gallo, P. Q., Pampanin, S., & Bergmeister, K. (2020). Seismic demands on non-structural components anchored to concrete accounting for structure-fastener-non-structural interaction (SFNI). *Earthquake Engineering and Structure and Dynamics*, *49*, 589-606. https://doi.org/10.1002/eqe.3255

[10] Villaverde, R. (1997). Seismic Design of Secondary Structures: State of the Art. *Journal of Structural Engineering*, *123*(8), 1011-1019. https://doi.org/10.1061/(ASCE)0733-9445(1997)123:8(1011)

[11] Pantelies, C. P., Truman, K. Z., Behr, R. A., & Belarbi, A. (1996). Development of a loading history for seismic testing of architectural glass in a shop-front wall system. *Engineering Structures*, *18*(12), 917-935. https://doi.org/10.1016/0141-0296(95)00224-3

[12] Sucuoğlu, H. & Vallabhan, C. V. G. (1997). Behaviour of window glass panels during earthquakes. *Engineering Structures*, *19*(8), 685-694. https://doi.org/10.1016/S0141-0296(96)00130-7

[13] Xue, Q., Wu, C. W., Chen, C. C., & Chen, K. C. (2008). The draft code for performance-based seismic design of buildings in Taiwan. *Engineering Structures*, *30*, 1535-1547. https://doi.org/10.1016/j.engstruct.2007.10.002

[14] Ji, X., Liu, D., & Hutt, C. M. (2018). Seismic performance evaluation of a high-rise building with novel hybridcoupled walls. *Engineering Structures*, *169*, 216-225. https://doi.org/10.1016/j.engstruct.2018.05.011

[15] Smith, A. & Vance, V. (1996). Model to incorporate architectural walls in structural analyses. *Journal of Structural Engineering*, *122*, 431-438. https://doi.org/10.1061/(ASCE)0733-9445(1996)122:4(431)

[16] Vance, V. L. & Smith, H. A. (1996). *Effects of Architectural Walls on Building Response to Ambient and Seismic Excitations*. John A. Blume Earthquake Engineering Center Technical Report 117. Stanford Digital Repository.

[17] Derakhshan, H., Walsh, K. Q., Ingham, J. M., Griffith, M. C., & Thambiratnam, D. P. (2019). Seismic fragility assessment of non-structural components in unreinforced clay brick masonry buildings. *About Earthquake Engineering and Structural Dynamics*, *49*, 285-300. https://doi.org/10.1002/eqe.3238

[18] Pardalopoulos, S. I. & Pantazopoulou, S. J. (2015). Seismic response of non-structuralcomponents attached on multistorey buildings. *About Earthquake Engineering and Structural Dynamics*, *44*, 139-158. https://doi.org/10.1002/eqe.2466

[19] Merino, R. J., Perrone, D., & Filiatrault, A. (2020). Consistent floor response spectra for performance-based seismic design of non-structural elements. *About Earthquake Engineering and Structural Dynamics*, *49*, 261-284. https://doi.org/10.1002/eqe.3236

[20] Obando, J. C. & Lopez-Garcia, D. (2018). Inelastic Displacement Ratios for Nonstructural Components Subjected to Floor Accelerations. *Journal of Earthquake Engineering*, *22*, 569-594. https://doi.org/10.1080/13632469.2016.1244131

[21] Anajafi, H. & Medina, R. A. (2017). Evaluation of ASCE 7 equations for designing acceleration-sensitive nonstructural components using data from instrumented buildings. *About Earthquake Engineering and Structural Dynamics*, *47*(4), 1075-1094. https://doi.org/10.1002/eqe.3006

[22] Anajafi, H., Medina, R. A., & Santini-Bell, E. (2020). Inelastic foor spectra for designing anchored acceleration-sensitive nonstructural components. *Bulletin of Earthquake Engineering*, *18*, 2115-2147. https://doi.org/10.1007/s10518-019-00760-8

[23] M.eeri, S. B., Ciurlanti, J., & M.eeri, S. P. (2020). Comparison of traditional vs low-damage structural and non-

structural building systems through a cost/performance-based evaluation. *Earthquake Spectra*, *37*(1), 366-385. https://doi.org/10.1177/8755293020952445

[24] Sullivan, T. J. (2020). Post-Earthquake Reparability of Buildings: The Role of Non-Structural Elements. *Structural Engineering International*, *30*(2), 217-223. https://doi.org/10.1080/10168664.2020.1724525

[25] Qi, L., Kurata, M., Ikeda, Y., Kunitomo, K., & Takaoka, M. (2021). Seismic evaluation of two-elevation ceiling system by shake table tests. *About Earthquake Engineering and Structural Dynamics*, *50*, 1147-1166. https://doi.org/10.1002/eqe.3390

[26] Perrone, D., Calvi, P. M., Nascimbene, R., Fischer, E. C., & Magliulo, G. (2019). Seismic performance of non-structural elements during the 2016 Central Italy earthquake. *Bulletin of Earthquake Engineering*, *17*, 5655-5677. https://doi.org/10.1007/s10518-018-0361-5

[27] Baird, A. & Ferner, H. (2017). Damage to Non-Structural Elements in the 2016 Kaikōura Earthquake. *Bulletin of the New Zealand Society for Earthquake Engineering*, *50*(2), 187-193. https://doi.org/10.5459/bnzsee.50.2.187-193

[28] Isik, E., Aydin, M. C., & Buyuksarac, A. (2020). 24 January 2020 Sivrice (Elazig)earthquake damages and determination of earthquake parameters in the region. *Earthquakes and Structures*, *19*(2),145-156. https://doi.org/10.12989/eas.2020.19.2.145

[29] Yurdakul, Ö., Duran, B., Tunaboyu, O., & Avşar, Ö. (2021). Field reconnaissance on seismic performance of RC buildings after the January 24, 2020 Elazığ-Sivrice earthquake. *Natural Hazards*, *105*, 859-887. https://doi.org/10.1007/s11069-020-04340-x

[30] Aksoylu, C. & Arslan, M. H. (2021). Comparative Investigation of Different Earthquake Load Calculation Methods for Reinforced Concrete Buildings in the 2007 and 2019 Codes. *International Journal of Engineering Research and Development*, *13*(2), 359-374. https://doi.org/10.29137/umagd.844186

[31] Işık, E., Büyüksaraç, A., Ekinci, Y. L., Aydın, M. C., & Harirchian, E. (2020). The Effect of Site-Specific Design Spectrum on Earthquake-Building Parameters: A Case Study from the Marmara Region (NW Turkey). *Applied Sciences*, *10*(20), 7247. https://doi.org/10.3390/app10207247

[32] Aksoylu, C., Mobark, A., Hakan Arslan, M., & Hakkı Erkan, İ. (2020). A comparative study on ASCE 7-16, TBEC-2018 and TEC-2007 for reinforced concrete buildings. *Revista de la construcción*, *19*(2), 282-305. https://doi.org/10.7764/rdlc.19.2.282-305.

[33] Keskin, E., & Bozdoğan, K. B. (2018). 2007 ve 2018 Deprem Yönetmeliklerinin Kırklareli İli Özelinde Değerlendirilmesi. *Kırklareli University Journal of Engineering and Science*, *4*(1), 74-90.

[34] Yalın, M. & Ulutaş, H. (2021). Mevcut okul türü bir binanın deprem performansının 2007 ve 2018 deprem yönetmeliklerine göre değerlendirilmesi. *Niğde Ömer Halisdemir University Journal of Engineering Sciences*, *10*(2), 648-661. https://doi.org/10.28948/ngumuh.896637

[35] Atmaca, N., Atmaca, A., & Kılçık, S. (2019). Comparison of 2018 And 2007 Turkish Earthquake Regulations. *The International Journal of Energy and Engineering Sciences*, *4*(2), 19-25. https://doi.org/10.4274/tnd.galenos.2018.69335

[36] Işık, E., Ekinci, Y. L., Sayil, N., Buyuksarac, A., & Aydin, M. C. (2021). Time-dependent model for earthquake occurrence and effects of design spectra on structural performance: a case study from the North Anatolian Fault Zone, Turkey. *Turkish Journal of Earth Sciences*, *30*(2), 215-234. https://doi.org/10.3906/yer-2004-20

[37] Özer, Ö. &Yüksel, B. (2020) Deprem Etkilerinin Betonarme Çerçeveler İle Boşluklu Betonarme Perdeler Tarafından Birlikte Karşılandığı Yüksek Binaların Analiz Sonuçlarının TBDY, (2018) ve DBYBHY (2007) 'ye Göre

Karşılaştırılması. *Nigde Omer Halisdemir University Journal of Engineering Sciences*, *9*(2), 931-945. https://doi.org/10.28948/ngumuh.694781

[38] TBEC-2018. Turkish Building Earthquake Code; T. C. Resmi Gazete: Ankara, Turkey, 2018.

[39] CSI (Computers and Structures Inc.). SAP2000 v20 Analysis Reference Manual. CSI, Berkeley, 2020.

[40] AFAD (Afet ve Acil Durum Yönetimi Başkanlığı). See https://tdth.afad.gov.tr.

[41] See https://www.adatavir.com/sakarya-bu-depremlerle-yikildi-buyuk-acilar.html.

[42] Karalar, M. & Çavuşli, M. (2020). Assessing 3D Earthquake Behaviour of Nonstructural Components Under Eurocode 8 Standard. *The 2020 Structures Congress (Structures20).*

[43] Karalar, M. & Çavuşli, M. (2020). Assessing of Earthquake Performance of Nonstructural Components Considering 2018 International Building Code. *The 2020 Structures Congress (Structures20).*

[44] Cavuslu, M. (2022). *Seismic Designing of Non-structural Components Considering Shake Table Test and 3D Modelling*. Zonguldak Bulent Ecevit University, Institute of Science, Doctoral Thesis.

Contact information:

Memduh KARALAR
Zonguldak Bulent Ecevit University,
Department of Civil Engineering
E-mail: memduhkaralar@beun.edu.tr

Murat CAVUSLU
(Corresponding author)
Zonguldak Bulent Ecevit University,
Department of Civil Engineering
E-mail: murat.cavusli@beun.edu.tr

Necati MERT
Sakarya University,
Department of Civil Engineering
E-mail: mert@sakarya.edu.tr